

## Supporting Information

### Boosting photoelectrochemical performance on $\alpha$ -Ga<sub>2</sub>O<sub>3</sub> nanowire arrays by indium cation doping for self-powered ultraviolet detection

Junjun Xue<sup>1, ‡</sup>, Jiyuan Huang<sup>1, ‡</sup>, Kehan Li<sup>2</sup>, Ping Liu<sup>2</sup>, Yan Gu<sup>3</sup>, Ting Zhi<sup>1</sup>, Yan Dong<sup>4, †</sup>, and Jin Wang<sup>1, †</sup>

<sup>1</sup>College of Electronic and Optical Engineering and College of Flexible Electronics (Future Technology), Nanjing University of Posts and Telecommunications, Nanjing 210023, China

<sup>2</sup>School of Science, Nanjing University of Posts and Telecommunications, Nanjing 210023, China

<sup>3</sup>College of Integrated Circuit Science and Engineering (College of Industry-Education Integration), Nanjing University of Posts and Telecommunications, Nanjing 210023, China

<sup>4</sup>School of Electronic Engineering, Heilongjiang University, Harbin, 150080, China

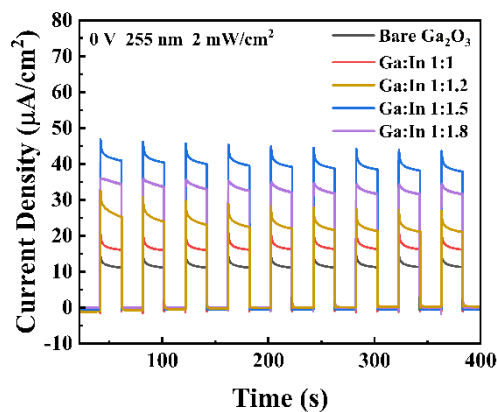


Fig. S1. (Color online) Current density–time curves of samples with different indium doping ratios.

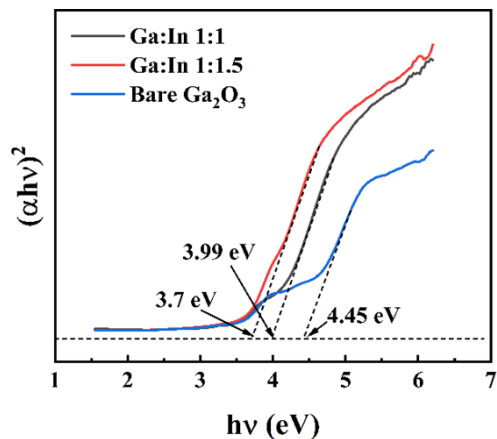


Fig. S2. (Color online) Tauc plots of the three sample groups.

The Tauc plot is used to determine the band gap energy ( $E_g$ ) of a material by plotting the relationship between the absorption coefficient ( $\alpha$ ) and photon energy ( $h\nu$ ). The band gap energy is typically determined by extrapolating the linear portion of the plot. The expression for the Tauc plot is:

$$(\alpha h \nu)^2 = A(h \nu - E_g) \quad \text{S1}$$

Where  $\alpha$  is the absorption coefficient,  $h$  is Planck's constant,  $\nu$  is the frequency of the incident light,  $E_g$  is the bandgap energy, and  $A$  is a constant.

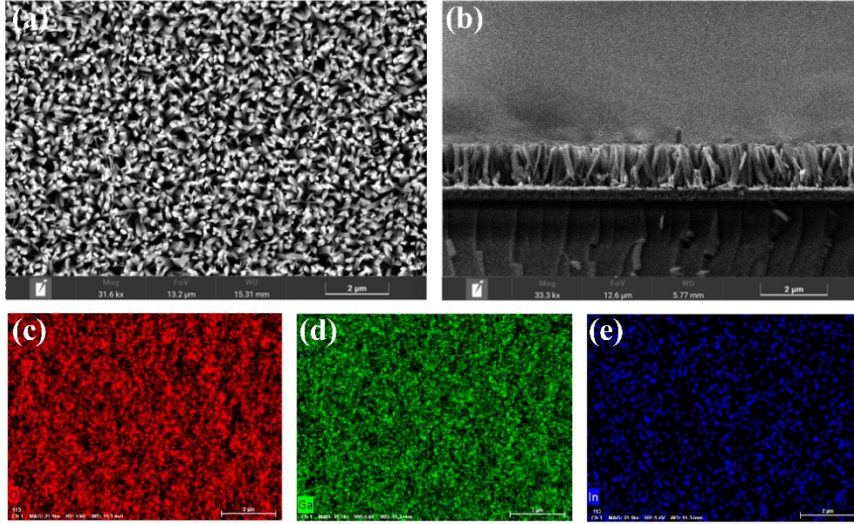


Fig. S3. (Color online) (a) Top-view scanning electron microscopy (SEM) image of indium-doped  $\alpha$ -Ga<sub>2</sub>O<sub>3</sub> samples. (b) Cross-sectional SEM image of indium-doped  $\alpha$ -Ga<sub>2</sub>O<sub>3</sub> samples. (c) Oxygen (O) elemental mapping of the indium-doped samples. (d) Gallium (Ga) elemental mapping of the indium-doped samples. (e) Indium (In) elemental mapping of the indium-doped samples.

Table S1. Performance Comparison of Ga<sub>2</sub>O<sub>3</sub>-based Ultraviolet Photodetectors from Previous Reports.

Structures	Type	Light condition	R(mA/W)	$\tau_{\text{rise}}/\tau_{\text{decay}}$ (ms)	Ref
$\beta$ -Ga <sub>2</sub> O <sub>3</sub>	PEC PD	254 nm	3.81	290/160	[1]
$\alpha$ -Ga <sub>2</sub> O <sub>3</sub>	PEC PD	254 nm	0.21	76/56	[2]
Al: $\alpha$ -Ga <sub>2</sub> O <sub>3</sub>	PEC PD	260 nm	1.46	421/139	[3]
$\alpha$ -Ga <sub>2</sub> O <sub>3</sub> /CFP	PEC PD	254 nm	12.9	150/130	[4]
$\alpha$ -Ga <sub>2</sub> O <sub>3</sub> - $\gamma$ -Al <sub>2</sub> O <sub>3</sub>	PEC PD	254 nm	0.174	100/100	[5]
$\alpha$ -Ga <sub>2</sub> O <sub>3</sub> /Cu <sub>2</sub> O QDs	PEC PD	254 nm	4.57	810/970	[6]
$\alpha$ -GaOOH/ $\alpha$ -Ga <sub>2</sub> O <sub>3</sub>	PEC PD	250 nm	0.29	240/60	[7]
$\alpha$ -Ga <sub>2</sub> O <sub>3</sub> /ZnS	PEC PD	310 nm	12.9	59/18	[8]
SnO <sub>2</sub> / $\alpha$ -Ga <sub>2</sub> O <sub>3</sub>	PEC PD	265 nm	5.94	17/18	[9]
$\alpha$ -Ga <sub>2</sub> O <sub>3</sub> /ZnO	PEC PD	254 nm	34.2	250/180	[10]
$\alpha$ -Ga <sub>2</sub> O <sub>3</sub>	PEC PD	255 nm	11.75	54/11	this work
In: $\alpha$ -Ga <sub>2</sub> O <sub>3</sub>	PEC PD	255 nm	38.85	13/8	this work

## Reference

- [1] Chen K, Wang S L, He C R, et al. Photoelectrochemical self-powered solar-blind photodetectors based on Ga<sub>2</sub>O<sub>3</sub> nanorod array/electrolyte solid/liquid heterojunctions with a large separation interface of photogenerated carriers. *ACS Appl Nano Mater*, 2019, 2(10), 6169
- [2] Zhang J H, Jiao S J, Wang D B, et al. Solar-blind ultraviolet photodetection of an  $\alpha$ -Ga<sub>2</sub>O<sub>3</sub> nanorod array based on photoelectrochemical self-powered detectors with a simple, newly-designed structure. *J Mater Chem C*, 2019, 7(23), 6867
- [3] Guo J C, Sun G W, Fan M M, et al. Hydrothermal growth of an Al-Doped  $\alpha$ -Ga<sub>2</sub>O<sub>3</sub> nanorod array and its application in self-powered solar-blind UV photodetection based on a photoelectrochemical cell. *Micromachines*, 2023, 14(7), 1336
- [4] Huang L J, Hu Z R, Zhang H, et al. A simple, repeatable and highly stable self-powered solar-blind photoelectrochemical-type photodetector using amorphous Ga<sub>2</sub>O<sub>3</sub> films grown on 3D carbon fiber paper. *J Mater Chem C*, 2021, 9(32), 10354
- [5] Zhang J H, Jiao S J, Wang D B, et al. Nano tree-like branched structure with  $\alpha$ -Ga<sub>2</sub>O<sub>3</sub> covered by  $\gamma$ -Al<sub>2</sub>O<sub>3</sub> for highly efficient detection of solar-blind ultraviolet light using self-powered photoelectrochemical method. *Appl Surf Sci*, 2021, 541, 148380
- [6] Han P P, Kang T X, Chen W H, et al. Cu<sub>2</sub>O quantum dots modified  $\alpha$ -Ga<sub>2</sub>O<sub>3</sub> nanorod arrays as a heterojunction for improved sensitivity of self-powered photoelectrochemical detectors. *J Alloys Compd*, 2023, 952, 170063
- [7] Zhang Y A, Jiao S J, Zhang J H, et al. Study on the evolution from  $\alpha$ -GaOOH to  $\alpha$ -Ga<sub>2</sub>O<sub>3</sub> and solar-blind detection behavior of an  $\alpha$ -GaOOH/ $\alpha$ -Ga<sub>2</sub>O<sub>3</sub> heterojunction. *CrystEngComm*, 2022, 24(9), 1789
- [8] Chang Y Y, Fan M M, Xu X J, et al. A fast-speed self-powered ZnS nanoparticles/ $\alpha$ -Ga<sub>2</sub>O<sub>3</sub> nanorod array/FTO UV photodetector based on a photoelectrochemical cell for outdoor UV detection. *Chem Phys Lett*, 2023, 832, 140879
- [9] Chen H Y, Huang Y C, Yao R H, et al. High-responsivity photoelectrochemical ultraviolet photodetector based on SnO<sub>2</sub> nanosheets-Ga<sub>2</sub>O<sub>3</sub>. *J Phys D: Appl Phys*, 2024, 58(2), 025103
- [10] Liu W J, Deng J R, Zhang D, et al. Construction of  $\alpha$ -Ga<sub>2</sub>O<sub>3</sub>-ZnO heterojunction for a promoted performance applied in self-powered solar blind photodetector. *Eur Phys J Appl Phys*, 2022, 97, 57